

Electrical resistivity, thermopower and thermal conductivity studies of $(\text{Sm}_{1-x}\text{Y}_x)\text{Cu}_2$ and RCu_2 (R identical to Gd, Pr or Tb) systems

This article has been downloaded from IOPscience. Please scroll down to see the full text article.

1993 J. Phys.: Condens. Matter 5 6737

(<http://iopscience.iop.org/0953-8984/5/36/028>)

View [the table of contents for this issue](#), or go to the [journal homepage](#) for more

Download details:

IP Address: 171.66.16.96

The article was downloaded on 11/05/2010 at 01:44

Please note that [terms and conditions apply](#).

Electrical resistivity, thermopower and thermal conductivity studies of $(\text{Sm}_{1-x}\text{Y}_x)\text{Cu}_2$ and RCu_2 ($\text{R} \equiv \text{Gd}, \text{Pr}$ or Tb) systems

C S Garde, J Ray and G Chandra

Tata Institute of Fundamental Research, Homi Bhabha Road, Bombay 400005, India

Received 11 May 1993

Abstract. We report the electrical resistivity ρ , thermopower S and thermal conductivity λ studies of $(\text{Sm}_{1-x}\text{Y}_x)\text{Cu}_2$ and RCu_2 ($\text{R} \equiv \text{Gd}, \text{Pr}$ or Tb) systems between 4.2 and 300 K. The value of the antiferromagnetic ordering temperature T_N for the $(\text{Sm}_{1-x}\text{Y}_x)\text{Cu}_2$ systems is found to become depressed, almost linearly, with Y substitution. The value of T_N extrapolates to zero as $x \rightarrow 1$. Such a behaviour is attributed solely to the dilution effects of Sm by Y atoms. Chemical pressure effects on the value of T_N due to addition of Y atoms are found to be negligible. The λ curves of SmCu_2 , GdCu_2 and TbCu_2 exhibit a peak for $T < T_N$. This low-temperature peak, at $T_{\text{max}}^{\lambda} \simeq 10$ K, in the λ data of these compounds arises from the combined influence of the electronic and the magnetic contribution to the total λ . This low-temperature peak becomes suppressed for $x \geq 0.10$. The S curves exhibit several extremum features, at $T \leq T_N$, which is ascribed to the variation in the density of states at the Fermi level.

Recently, there has been renewed interest [1–4] in the study of the RCu_2 ($\text{R} \equiv$ rare earth elements) types of compound. These compounds exhibit a complex magnetic behaviour at low temperatures ($T < 60$ K). CeCu_2 is found to exhibit [5] a magnetic Kondo-lattice behaviour, whereas EuCu_2 and YbCu_2 show [1] mixed-valency (MV) features as revealed from the lattice constant studies. The other RCu_2 compounds ($\text{R} \equiv \text{Sm}, \text{Nd}, \text{Gd}, \text{Tb}, \text{Dy}, \text{Ho}, \text{Er}$ or Tm) are found to exhibit [3, 4, 6–8] an antiferromagnetic (AF) transition for $T_N < 60$ K. At still lower temperatures, some of the compounds such as RCu_2 ($\text{R} \equiv \text{Dy}, \text{Er}, \text{Tb}$ or Nd) show [2, 7] the evolution of another magnetic transition, related to spin reorientation effects within the already-developed AF phase, at a temperature $T_m < T_N$. This has been essentially revealed through neutron studies [3, 7]. For example, for HoCu_2 , the longitudinally modulated spin structure below $T_N (\simeq 10$ K) changes to a transversely modulated structure below $T_m \simeq 7$ K, whereas TbCu_2 reveals a longitudinally modulated structure below $T_N \simeq 55$ K, which transforms to a collinear AF structure below $T_m \simeq 47$ K. The magnetic structures of ErCu_2 and TmCu_2 are also found to change below T_N , although their exact nature could not be determined even from the neutron studies. The low-temperature magnetic phase of the RCu_2 compounds is thus found to be quite complex.

For SmCu_2 also, the occurrence of two magnetic transitions at temperatures $T_N = 23$ K and $T_m = 17$ K has been inferred from the specific heat C , the magnetic susceptibility χ and the thermal expansion α data. However, no neutron studies have so far been carried out on this compound. Initial transport studies [1] on SmCu_2 have also been found to be quite interesting. The ρ studies showed evidence of these two transitions at temperatures T_N^{ρ} and T_m^{ρ} close to those derived from the magnetic studies. At still lower temperatures ($T \simeq 10$ K) the λ data show a sharp peak whose origin is not well understood yet. In view

of these complex magnetic and transport behaviours, we have studied the $(\text{Sm}_{1-x}\text{Y}_x)\text{Cu}_2$ ($x = 0, 0.05, 0.1, 0.3, 0.6$ and 1) alloys. As the Y atoms are smaller than the Sm atoms, the substitution of Sm by Y would lead to a decrease in the unit-cell volume, thus giving rise to a positive chemical pressure. As Sm is found to exhibit [9] MV features as a result of chemical pressure effects induced by Y substitution in alloys such as $\text{Sm}_{1-x}\text{Y}_x\text{S}$ or because of an externally applied pressure as in SmB_6 and SmSb , it would be interesting to investigate whether such MV tendencies would develop also in the $(\text{Sm}_{1-x}\text{Y}_x)\text{Cu}_2$ alloys. Secondly, our substitution studies would enable us to study the variations in T_N^ρ and T_m^ρ , with x , over the pure SmCu_2 ($x = 0$) case. Thirdly, the substitution of Sm by Y in SmCu_2 alloy would also enable us to study the effect on the low-temperature peak, at T_{max}^λ , in the λ curve. Finally, TbCu_2 , GdCu_2 and PrCu_2 alloys have also been studied to compare their low-temperature transport properties with those of SmCu_2 .

Table 1. Lattice parameters and RRR ($= \rho(270 \text{ K})/\rho(5 \text{ K})$) values for $(\text{Sm}_{1-x}\text{Y}_x)\text{Cu}_2$ and RCu_2 ($\text{R} \equiv \text{Gd, Pr or Tb}$) systems.

System	a (Å)	b (Å)	c (Å)	V (Å ³)	RRR
SmCu_2	4.355 ± 0.007	6.929 ± 0.001	7.372 ± 0.001	222.5	41.2
$(\text{Sm}_{0.95}\text{Y}_{0.05})\text{Cu}_2$	4.353 ± 0.002	6.933 ± 0.003	7.365 ± 0.004	222.3	8.7
$(\text{Sm}_{0.9}\text{Y}_{0.1})\text{Cu}_2$	4.347 ± 0.003	6.933 ± 0.003	7.365 ± 0.006	222.0	6.4
$(\text{Sm}_{0.7}\text{Y}_{0.3})\text{Cu}_2$	4.341 ± 0.003	6.921 ± 0.004	7.350 ± 0.006	220.8	2.8
$(\text{Sm}_{0.4}\text{Y}_{0.6})\text{Cu}_2$	4.328 ± 0.001	6.906 ± 0.002	7.331 ± 0.003	219.1	2.8
YCu_2	4.290 ± 0.003	6.855 ± 0.004	7.271 ± 0.006	213.8	13.3
GdCu_2	4.329 ± 0.004	6.909 ± 0.005	7.346 ± 0.008	219.7	64.0
TbCu_2	4.318 ± 0.003	6.891 ± 0.004	7.326 ± 0.006	218.0	56.0
PrCu_2	4.410 ± 0.005	7.050 ± 0.007	7.454 ± 0.009	231.7	18.0

All the samples were prepared in an arc furnace under flowing argon conditions and repeatedly melted to ensure chemical homogeneity. All of them are found to crystallize in the orthorhombic CeCu_2 -type structure. The lattice parameters (table 1) for the SmCu_2 and RCu_2 ($\text{R} \equiv \text{Y, Tb, Gd or Pr}$) compounds are found to match well with the previously reported [1] values. For the $(\text{Sm}_{1-x}\text{Y}_x)\text{Cu}_2$ alloys, the values of the parameters a , b and c are found to decrease (table 1) monotonically from $x = 0$ (SmCu_2) to $x = 1$ (YCu_2). This is also reflected (table 1) in the decrease in the cell volume V . The residual resistivity ratio (RRR) (equals $\rho(270 \text{ K})/\rho(5 \text{ K})$) is found (table 1) to be 41.2, 13.3, 64, 56 and 18 for the SmCu_2 , YCu_2 , GdCu_2 , TbCu_2 and PrCu_2 compounds, respectively. The large values of RRR for these compounds indicate the good quality of our samples and are comparable with those reported earlier [10]. The decrease in the value (table 1) of RRR for the various $(\text{Sm}_{1-x}\text{Y}_x)\text{Cu}_2$ alloys arises owing to the random substitution of Sm by Y atoms. The annealing heat treatment (700 °C for 1 week) for the $(\text{Sm}_{1-x}\text{Y}_x)\text{Cu}_2$ alloys was found to improve negligibly the RRR values as obtained for the as-cast samples. The constancy of the RRR values with these heat treatments indicates that, with the variation in x , well formed solid solutions are obtained.

The ρ curves (figure 1) of all the $(\text{Sm}_{1-x}\text{Y}_x)\text{Cu}_2$ alloys exhibit a complex behaviour at low temperatures. SmCu_2 ($x = 0$) is found (figure 2) to show clear changes in slope ($\partial\rho/\partial T$) at temperatures of around 19 and 24 K. The change in slope at the higher temperature ($T = 24 \text{ K}$) is associated with the onset of the high-temperature AF phase detected from the magnetic studies [1]. We therefore take $T_N^\rho = 24 \text{ K}$. In contrast the change in slope at the lower temperature ($T = 19 \text{ K}$) has been associated with magnetic

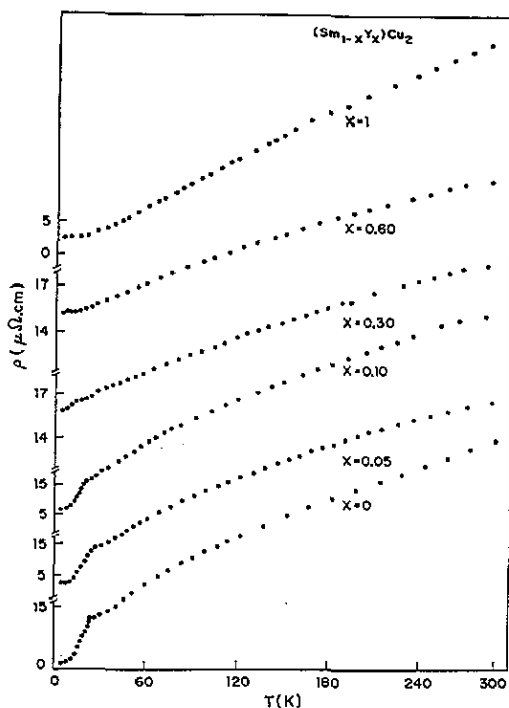


Figure 1. ρ versus T curves for the $(Sm_{1-x}Y_x)Cu_2$ systems.

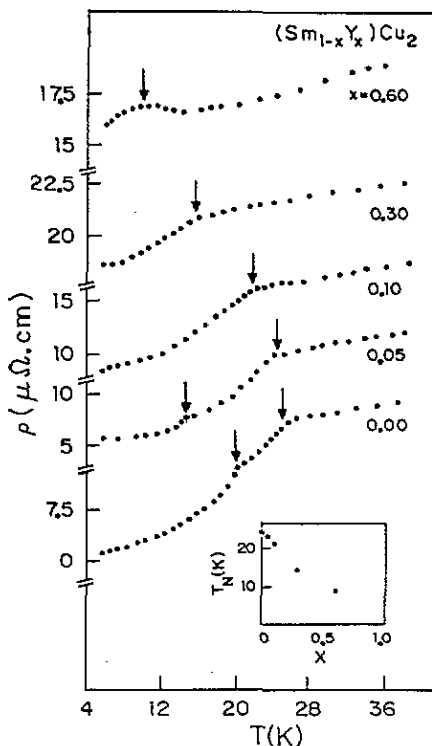


Figure 2. Low-temperature plots of ρ versus T for the $(Sm_{1-x}Y_x)Cu_2$ systems. The arrows indicate the temperatures at which the magnetic transitions occur. For the $x = 0$ and 0.05 alloys, the arrow at the lower temperature indicates T_m^ρ . The inset shows the variation in T_N^ρ with x .

spin reorientation effects of the Sm ions, as deduced from the χ and α studies [1]. In the same way, we take $T_m^\rho = 19$ K. These anomalies at T_N^ρ and T_m^ρ are seen more clearly in the expanded low-temperature plots (figure 2). With the increase in x in the $(Sm_{1-x}Y_x)Cu_2$ alloys, the value of T_N^ρ shifts (figure 2) to lower temperatures. Also T_N^ρ decreases (inset in figure 2) almost linearly with x and extrapolates to zero for $x \rightarrow 1$. This suggests that depression of T_N is mainly due to the magnetic dilution effects caused by the addition of Y ions. In general, the value of T_N is governed principally by the value of the Ruderman-Kittel-Kasuya-Yosida (RKKY) characteristic temperature scale T_{RKKY} given by the equation [11] $T_N \sim T_{RKKY} \sim cI^2$, where $c (= 1 - x)$ is the concentration of the Sm ions and I is the exchange integral between the Sm ions and the conduction electrons of the alloy. This relation shows that $T_N \rightarrow 0$ as $c \rightarrow 0$, as suggested by our experiments. Any other competing magnetic process would lead to a departure from the above-mentioned T_N depression. We thus conclude that MV effects are not found to develop by variation in x over the entire alloy series, and chemical pressure effects, which are known to induce [9] MV effects in alloys such as $Sm_{1-x}Y_xS$, are not important for the $(Sm_{1-x}Y_x)Cu_2$ alloys. The value of T_m^ρ is also found (table 2) to decrease from 19 K for $SmCu_2$ to 14 K for the $x = 0.05$ alloy. Thus, T_m^ρ also shows a tendency to decrease with increase in x . Such spin reorientation effects, at T_m^ρ are found to be barely visible (figure 2) for the $x \geq 0.1$ alloys.

Hence the value of T_m^ρ , for the $x \geq 0.1$ alloys, could not be determined from our studies. At high temperatures ($T > T_N$), the ρ curves (figure 1) of $(\text{Sm}_{1-x}\text{Y}_x)\text{Cu}_2$ alloys are found to increase monotonically with a tendency to saturate at high temperatures of around 300 K.

Table 2. Various characteristic temperatures for $(\text{Sm}_{1-x}\text{Y}_x)\text{Cu}_2$ and the magnetically ordered RCu_2 ($R \equiv \text{Gd}$ or Tb) systems. T_N is the value of the antiferromagnetic ordering temperature from magnetic studies [1, 6].

System	T_{\max}^λ (K)	T_m^ρ (K)	T_N (K)	T_N^ρ (K)	T_{\min}^λ (K)	T_{\max}^S (K)
SmCu_2	10	19	23 [1]	24	24	22
$(\text{Sm}_{0.95}\text{Y}_{0.05})\text{Cu}_2$	—	14	—	23	23	19
$(\text{Sm}_{0.9}\text{Y}_{0.1})\text{Cu}_2$	—	—	—	21	—	14
$(\text{Sm}_{0.7}\text{Y}_{0.3})\text{Cu}_2$	—	—	—	14	—	—
$(\text{Sm}_{0.4}\text{Y}_{0.6})\text{Cu}_2$	—	—	—	9	—	—
GdCu_2	10	—	40 [6]	40	40	25
TbCu_2	10	—	55 [6]	52	50	25

We now examine the S behaviour. The S curves (figure 3) of the $(\text{Sm}_{1-x}\text{Y}_x)\text{Cu}_2$ alloys exhibit a complex behaviour especially at low temperatures ($T < 40$ K). A maximum (S_{\max}) is observed (table 2) at $T_{\max}^S = 22$ K for the $0 \leq x \leq 0.3$ alloys, which is different from T_N^ρ (indicated by the arrow in figure 3). Such differences have also been observed [12] in many other systems. This extremum feature, in the S curve, at low temperatures arises [10] essentially because S depends sensitively on the variation in the density of states at the Fermi level and not because of the magnetic ordering effects at T_N . For the $x = 0.6$ alloy, a broad bend develops (figure 3) at $T \simeq 32$ K, instead of the maximum observed for the $x \leq 0.3$ alloys. For YCu_2 ($x = 1$), this bend also becomes very much reduced (figure 3), and the S curve shows an almost monotonic increase. For higher temperatures ($T > 25$ K), the alloys with x varying between 0 and 0.30 show a broad minimum at negative S -values. For $x > 0.30$, this negative minimum is no longer observed and the S curve becomes entirely positive. Such complex behaviour of the S data is not understood at present and is related to the different temperature dependencies of the electron diffusion and the phonon drag contributions to the total thermopower.

We now analyse the λ behaviour. The λ curve shows (figure 4) a minimum at a temperature T_{\min}^λ (table 2), for the $x = 0$ and 0.05 alloys close to the AF transition temperature T_N detected from the ρ and the χ measurements. At still lower temperatures ($T < T_{\min}^\lambda$), the λ curve for SmCu_2 alone is found (figure 4) to show a clear maximum at a characteristic temperature $T_{\max}^\lambda \simeq 10$ K. With increase in x , two striking aspects in the λ behaviour have been observed. Firstly, complete suppression of the low-temperature peak occurs with the addition of Y atoms ($x > 0$) to SmCu_2 . Secondly, for the $x > 0.10$ alloys, T_{\min}^λ is also no longer observed. Instead the AF transition now occurs at a temperature where the $\lambda(T)$ curve exhibits (figure 5) a change in slope. For the non-magnetic YCu_2 ($x = 1$) compound, the $\lambda(T)$ curve shows (figure 4) only a smooth behaviour with a broad peak at around 30 K.

The low-temperature $\lambda(T)$ behaviour of these alloys arises [13, 14] from the combined influence of the electronic, magnetic and phononic terms to the total λ . The result of this complex interplay is reflected (figure 6) in the temperature dependence of the Lorenz number $L(T) = \rho(T)\lambda(T)/T$. The maximum in the $L(T)$ curve occurs (figure 6) at almost the same temperature T_N^ρ as obtained from the ρ studies. For the non-magnetic YCu_2 ($x = 1$) system, this peak becomes very much reduced, indicating that this feature is mainly magnetic in origin. Such sharp features in the $L(T)$ curve, which are related to

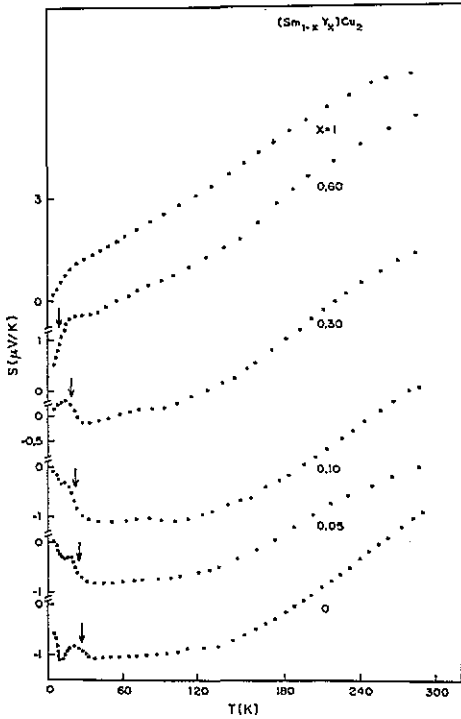


Figure 3. S versus T curves for the $(Sm_{1-x}Y_x)Cu_2$ systems. The arrows indicate the T_N^ρ -values obtained from our ρ studies.

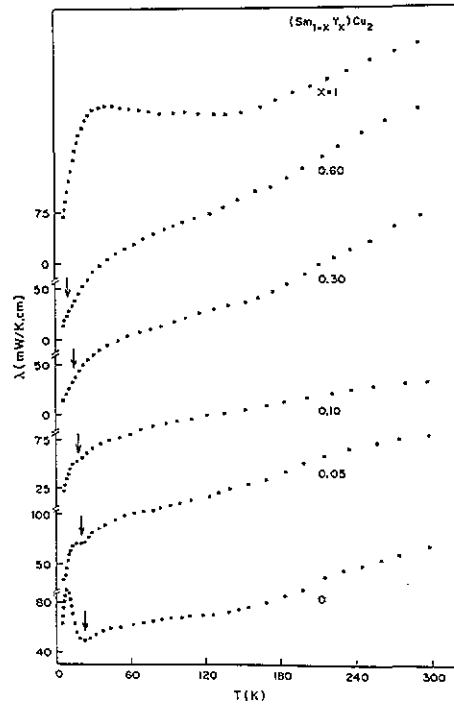


Figure 4. λ versus T curves for the $(Sm_{1-x}Y_x)Cu_2$ systems. The arrows indicate the T_N^ρ -values obtained from our ρ studies.

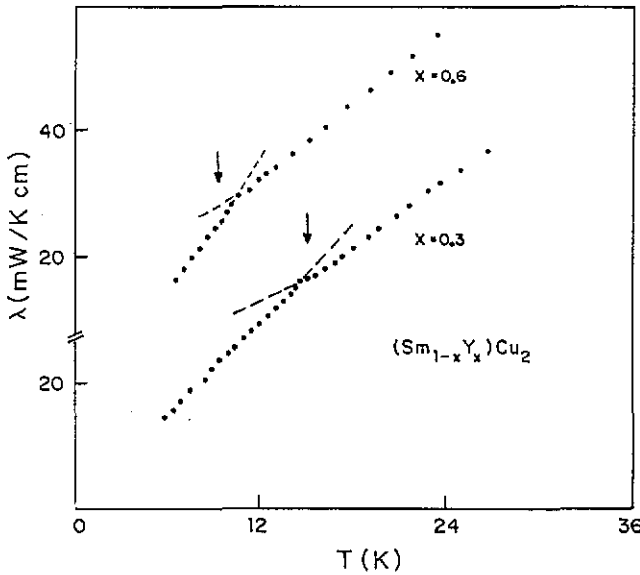


Figure 5. Low-temperature plots of λ versus T for the $(Sm_{1-x}Y_x)Cu_2$ ($x = 0.3$ and 0.6) systems. The arrows indicate the T_N^ρ -values obtained from our ρ studies. T_N^ρ is quite close to the temperature where the change in slope (highlighted by the broken lines) occurs in the λ curve.

the magnetic ordering effects, are not uncommon [15, 16] amongst the rare-earth metals. At higher temperatures, $L(T)$ decreases in value and approaches the free-electron value of

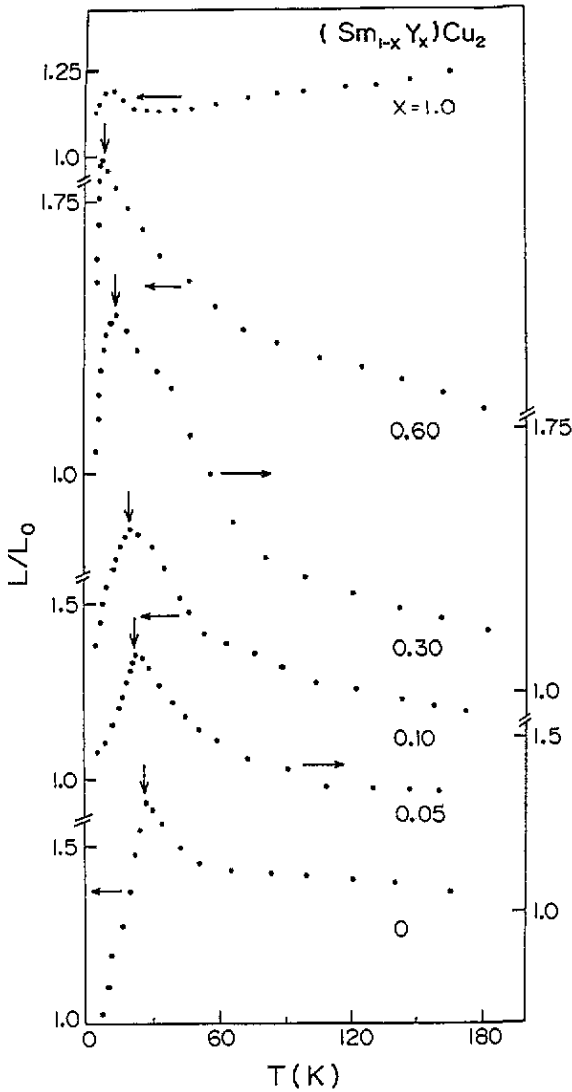


Figure 6. The plot of L/L_0 versus T for the $(\text{Sm}_{1-x}\text{Y}_x)\text{Cu}_2$ alloys. The vertical arrows indicate the T_N^0 -values obtained from our ρ studies. The horizontal arrows identify the appropriate y axis for these compounds.

$$L_0 = 2.45 \times 10^{-8} \text{ V}^2 \text{ K}^{-2}.$$

We now analyse the transport properties of the RCu_2 ($\text{R} \equiv \text{Gd}, \text{Pr}$ or Tb) alloys. A sudden change in the slope due to freezing out of the spin-disorder component in the ρ curve, at T_N^0 , is found (figure 7) to occur for GdCu_2 and TbCu_2 at 40 K and 52 K, respectively. Our values (table 2) are quite close [6,7] to $T_N = 40$ K and 55 K for the GdCu_2 and TbCu_2 compounds, respectively, obtained from the χ data. We note that no freezing of the spin-disorder component has been observed for the PrCu_2 compound down to 1.7 K, thus indicating that there is no evidence for the presence of any AF transition.

Another interesting feature of the RCu_2 series is that the value of T_N attains the maximum value for $\text{R} \equiv \text{Tb}$ with $T_N = 55$ K instead of for $\text{R} \equiv \text{Gd}$ with $T_N = 40$ K. This shows that the deGennes [17] scaling law is not applicable to this class of compounds. This scaling law predicts that, in the free-ion picture, T_N depends on J , where J is the total angular momentum of the magnetic ion. However, it has been shown [18,19] from theoretical calculations that the value of T_N could increase, over the deGennes value, owing to the

influence of the low-lying crystal-field (CF) states. Such effects of CF variation across the RCu_2 series could also be responsible for the situation $T_N(TbCu_2) > T_N(GdCu_2)$. A similar role of CF effects has been earlier evidenced [19] in the case of the RRh_4B_4 ($R \equiv Nd, Sm, Gd, Tb, Dy, Ho, Er$ or Tm) series, where T_N was found to be a maximum for the $R \equiv Dy$ compound. Some additional evidence for the CF effects is also reflected in the high-temperature ρ data. At high temperature ($T > T_N^\rho$), the ρ curve for $GdCu_2$ is found to be almost linear with temperature, whereas that for $PrCu_2$ and $TbCu_2$ is found to show (figure 7) a slight saturation effect at high temperatures ($T > 150$ K), similar to that seen (figure 1) also for $SmCu_2$. Such a high-temperature curvature, in the ρ curve, could be related to CF effects.

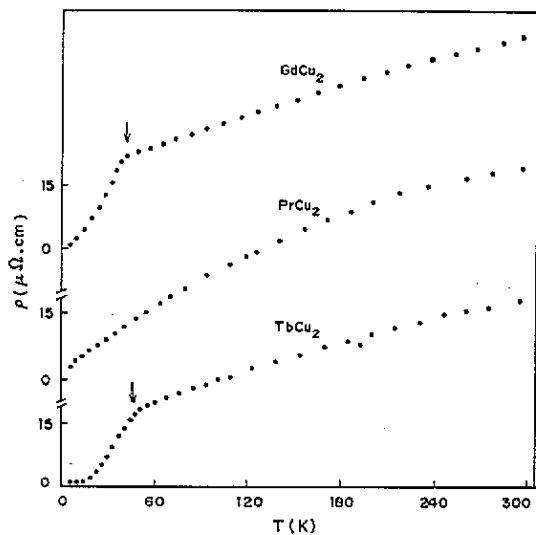


Figure 7. ρ versus T curves for the RCu_2 ($R \equiv Gd, Pr$ or Tb) compounds. The arrows indicate the temperatures at which the magnetic transitions occur. The curves for $PrCu_2$ and $TbCu_2$ show a slight curvature at high temperatures ($40 \text{ K} < T < 300 \text{ K}$) compared with the almost linear increase in ρ for $GdCu_2$.

The S curves (figure 8) for all the RCu_2 ($R \equiv Gd, Pr$ or Tb) compounds show features similar to that of $SmCu_2$ ($x = 0$). For the $GdCu_2$ and $TbCu_2$ compounds, T_N^ρ is not equal (table 2) to the temperature T_{max}^S (≈ 30 K) where S_{max} occurs but satisfies the condition $T_N^\rho > T_{max}^S$. Although $PrCu_2$ also reveals (figure 8) a maximum in the S curve, no evidence for the AF transition has been detected from the ρ studies. These observations show, as mentioned earlier, that the development of S_{max} is not directly related to the AF transition and pertains to the fact that the S behaviour depends sensitively on the derivative of the density of states at the Fermi level.

The λ curves (figure 9) of the RCu_2 ($R \equiv Gd, Pr$ or Tb) compounds are also found to show interesting behaviour. For both $TbCu_2$ and $GdCu_2$, $T_{max}^\lambda \approx 10$ K is found to be less than both T_{min}^λ and T_N^ρ . For $TbCu_2$, the maximum at T_{max}^λ is much more sharp and pronounced (figure 9) than for $GdCu_2$. At higher temperatures ($T > T_{min}^\lambda$), the λ curves for these alloys are found to increase monotonically from 60 to 300 K. The high-temperature behaviour is thus quite similar to that of $SmCu_2$. The λ curve of $PrCu_2$ does not show the low-temperature maximum but instead reveals a pronounced bend at around 30 K.

The main conclusions are summarized as follows. The depression of T_N in the $(Sm_{1-x}Y_x)Cu_2$ systems is mainly governed by the dilution of Sm by Y atoms. There is no evidence for the development of MV behaviour of Sm ions by variation in x . The values of T_N for the RCu_2 series of compounds could be influenced by the presence of CF effects. The low-temperature peak, at T_{max}^λ , in some of the λ curves of $(Sm_{1-x}Y_x)Cu_2$, $TbCu_2$ and

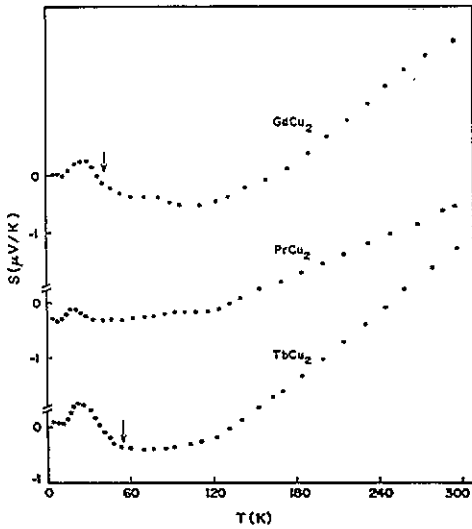


Figure 8. S versus T curves for the RCu_2 ($R \equiv Gd, Pr$ or Tb) compounds. The arrows indicate the T_N^ρ -values obtained from our ρ studies.

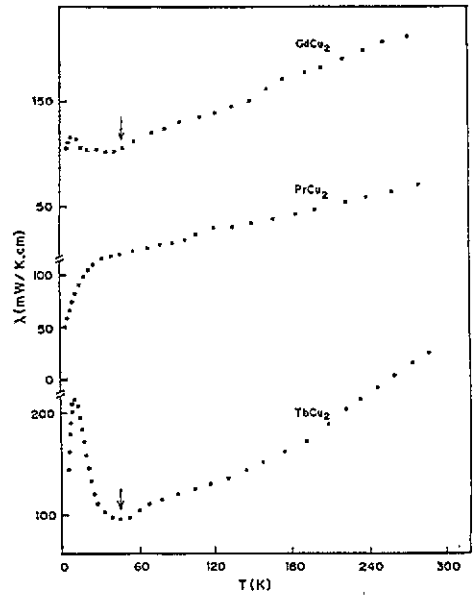


Figure 9. λ versus T curves for the RCu_2 ($R \equiv Gd, Pr$ or Tb) compounds. The arrows indicate the T_N^ρ -values obtained from our ρ studies.

$GdCu_2$ systems arises from the combined influence of the electronic and magnetic terms of the total thermal conductivity contribution.

References

- [1] Gratz E, Pillmayr N, Bauer E, Muller H, Barbara B and Loewenhaupt M 1990 *J. Phys.: Condens. Matter* **2** 1485
- [2] Gratz E, Loewenhaupt M, Divis M, Steiner W, Bauer E, Pillmayr N, Muller H, Nowotny H and Frick B 1991 *J. Phys.: Condens. Matter* **3** 9297
- [3] Lebech B, Smetana Z and Sima V 1987 *J. Magn. Magn. Mater.* **70** 97
- [4] Luong N H, Franse J J M and Hien T D 1985 *J. Magn. Magn. Mater.* **50** 153
- [5] Gratz E, Bauer E, Barbara B, Zemirli S, Steglich F, Bredl C D and Lieke W 1985 *J. Phys. F: Met. Phys.* **15** 1975
- [6] Sherwood R C, Williams H J and Wernick J H 1964 *J. Appl. Phys.* **35** 1049
- [7] Hashimoto Y, Fujii H, Fujiwara H and Okamoto T 1979 *J. Phys. Soc. Japan* **47** 67
- [8] Hashimoto Y, Fujii H, Fujiwara H and Okamoto T 1979 *J. Phys. Soc. Japan* **47** 73
- [9] Lawrence J M, Riseborough P S and Parks R D 1981 *Rep. Prog. Phys.* **44** 1
- [10] Gratz E and Zuckermann M J 1982 *Handbook on the Physics and Chemistry of Rare Earths* vol 5 ed K A Gschneidner Jr and L Eyring (Amsterdam: North-Holland) p 117
- [11] Brandt N B and Moschalkov V V 1984 *Adv. Phys.* **33** 373
- [12] Sakurai J, Yamaguchi Y, Mibu K and Shinjo Y 1990 *J. Magn. Magn. Mater.* **84** 157
- [13] Berman R 1979 *Thermal Conduction in Solids* (Oxford: Oxford University Press) p 121
- [14] Ziman J M 1960 *Electrons and Phonons* (Oxford: Oxford University Press) p 288
- [15] Edwards L R and Legvold S 1968 *Phys. Rev.* **176** 753
- [16] Nellis W J and Legvold S 1969 *Phys. Rev.* **180** 581
- [17] deGennes P G 1962 *J. Phys. Radium* **23** 510
- [18] Noakes D R and Shenoy G K 1982 *Phys. Lett.* **91A** 35
- [19] Dunlap B D, Hall L N, Beheroozi F, Crabtree G W and Niarchos D G 1984 *Phys. Rev. B* **29** 6244